Journal of
Synchrotron
Radiation

ISSN 0909-0495

Received 7 January 2008
Accepted 22 November 2008

Focusing synchrotron radiation using a polycapillary half-focusing X-ray lens for imaging

Tianxi Sun,[a,b,c] Meiling Zhang,[d] Zhiguo Liu,[a,b,c]* Zhiguang Zhang,[e] Gang Li,[f] Yongzhong Ma,[g] Xiaoguang Du,[a,b,c] Quanjie Jia,[f] Yu Chen,[f] Qingxi Yuan,[f] Wanxia Huang,[f] Peiping Zhu[f] and Xunliang Ding[a,b,c]

[a]The Key Laboratory of Beam Technology and Materials Modification of Ministry of Education, Beijing Normal University, Beijing 100875, People's Republic of China, [b]Institute of Low Energy Nuclear Physics, Beijing Normal University, Beijing 100875, People's Republic of China, [c]Beijing Radiation Center, Beijing 100875, People's Republic of China, [d]Qufu People's Hospital, Qufu 273100, People's Republic of China, [e]Department of Mechanical and Electrical Engineering, Shandong Water Polytechnic, Rizhao 276826, People's Republic of China, [f]Synchrotron Radiation Laboratory, Institute of High Energy Physics, Chinese Academy of Science, Beijing 100039, People's Republic of China, and [g]Center for Disease Control and Prevention of Beijing, Beijing 100013, People's Republic of China. E-mail: liuzhiguo512@hotmail.com

An imaging system based on a polycapillary half-focusing X-ray lens (PHFXRL) and synchrotron radiation source has been designed. The focal spot size and the gain in power density of the PHFXRL were 22 μm (FWHM) and 4648, respectively, at 14.0 keV. The spatial resolution of this new imaging system was better than 5 μm when an X-ray charge coupled device with a pixel size of 10.9 × 10.9 μm was used. A fossil of an ancient biological specimen was imaged using this system.

Keywords: polycapillary X-ray optics; imaging.

1. Introduction

Improving spatial resolution is very important in imaging technology. When synchrotron radiation is used as the source, the required spatial resolution of the detector system is generally high because the small divergence of synchrotron radiation is not convenient for magnifying the image of the sample. There are various methods for decreasing the requirement on the spatial resolution of the detector system. For example, the X-ray image may first be converted into a visible-light image using a scintillating crystal screen, and then this visible-light image is recorded at a high spatial resolution using a visible-light detection system. As another example, the X-ray image may first be magnified using focusing X-ray optics (Mokso *et al.*, 2007; Piestrup *et al.*, 2005; Gary *et al.*, 2007; Ollinger *et al.*, 2007), and then this magnified image is recorded using an X-ray detection system with a relatively low spatial resolution. There are many focusing X-ray optics which can be used to focus a quasi-parallel synchrotron radiation beam into a spot with high flux density for magnifying the X-ray image, such as a zone plates, refractive X-ray lenses, Kirkpatrick–Baez mirrors, polycapillary X-ray optics, namely the Kumakhov lens (Dabagov *et al.*, 1995), and others. Fabrication of polycapillary X-ray optics is simple and, moreover, polycapillary X-ray optics has been used expediently to focus synchrotron radiation in micro X-ray analysis such as micro X-ray fluorescence, micro X-ray-absorption-fine-structure analyses (Janssensa *et al.*, 2004; Woll *et al.*, 2006; Sun *et al.*, 2006; Bulska *et al.*, 2006) and others.

In this paper a polycapillary half-focusing X-ray lens (PHFXRL) is proposed for focusing the quasi-parallel synchrotron radiation beam for imaging, and the performances of this system are studied in detail. As an example of its application, an ancient fossil has been imaged using this system.

2. Experiments and results

2.1. Experimental set-up

The experiments were carried out at beamline 4W1A at the Beijing Synchrotron Radiation Facility of China. Fig. 1 schematically shows the realisation of the imaging system based on the PHFXRL. A synchrotron radiation beam of diameter 2500 μm was focused into a microfocal spot of diameter 22 μm FWHM by using the PHFXRL at 14.0 keV. The size of a pixel of the CCD is 10.9 × 10.9 μm. The length, entrance diameter and exit diameter of the PHFXRL are 49.7, 5.0 and 2.9 mm, respectively. The number of capillaries composing the PHFXRL is 293000. The wall thickness of a monocapillary ranges from 0.2 to 0.3 μm, and the inner diameter ranges from 1 to 6 μm. The taper angle of a monocapillary ranges from 110 to 120 mrad.

2.2. Performances of the PHFXRL for imaging experiments

It is well known that the polycapillary X-ray optics is based on X-ray total external reflection. The critical angle of the total reflection is roughly determined by the X-ray energy *via* (for the borosilicate glass capillary used in our laboratory)

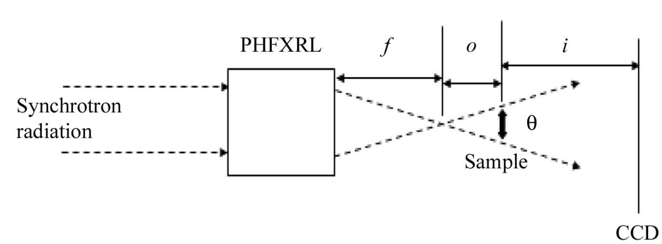

Figure 1
Scheme of the imaging system based on the PHFXRL.

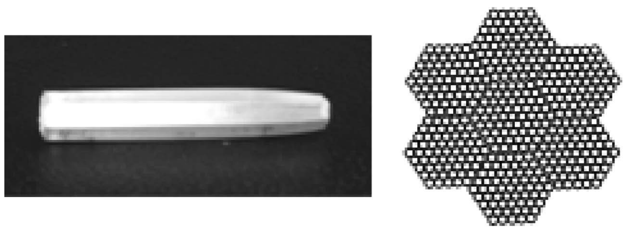

(*a*) (*b*)

Figure 2
Photograph of the PHFXRL (*a*) and sketch of part of the cross section (*b*).

$$\theta_{\rm c} \simeq \frac{30}{E\,({\rm keV})}\ {\rm mrad}, \qquad (1)$$

where E is the photon energy in keV. A photograph of the PHFXRL used in our experiments is shown in Fig. 2(*a*). As shown in Fig. 2(*b*), the PHFXRL is made of many compound polycapillaries of hexagonal shape, and in each compound polycapillary there are many monocapillaries.

The PHFXRL can focus a quasi-parallel X-ray beam into a microfocal spot (Sun *et al.*, 2007). Fig. 3 shows the energy dependence of the focal spot size and gain in flux density in the focal spot for the PHFXRL used in our experiments. The focal spot size of the PHFXRL was measured using the knife-edge scanning method, where a sharp knife-edge is moved across the beam focused by the PHFXRL and the focal spot size is measured as the FWHM of the differentiated knife-edge scan (Sun & Ding, 2004). As shown in Fig. 3, the focal spot size of the PHFXRL decreases with increasing energy. This mainly results from the decrease of the critical angle with increasing energy (Sun & Ding, 2005). The microfocal spot of the PHFXRL was convenient for improving the spatial resolution of the imaging system. The high gain of the PHFXRL was helpful in decreasing the imaging time. The focal distance f (see Fig. 1) of the PHFXRL was 12.81 mm and 12.90 mm at 8.5 keV and 16.5 keV, respectively. The calculated values of the energy dependence of the divergence θ (see Fig. 1) of the beam after the focal spot of the PHFXRL are shown in Fig. 4. With increasing energy the focal distance increases and the divergence decreases. This is explained by the well known $1/E$ energy dependence of the critical angle of total reflection of X-rays. The relatively large divergence of the beam after the focal spot of the PHFXRL was helpful in magnifying the X-ray image of the object. The increase in the focal distance of the PHFXRL with increasing energy was very small. This will be an advantage when the PHFXRL is used to focus the continuous X-ray spectrum for imaging.

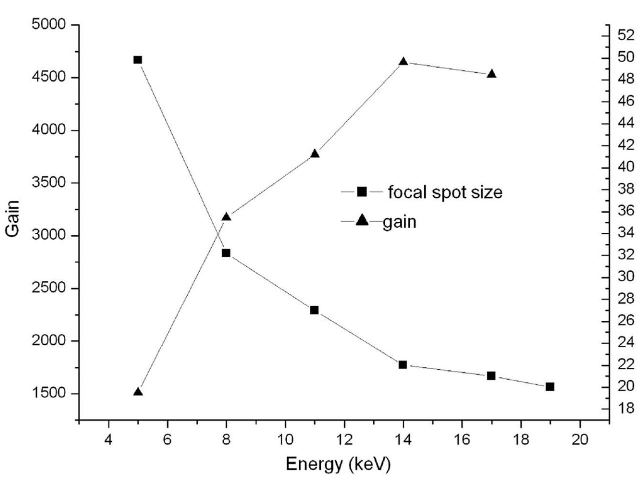

Figure 3
Energy dependence of the focal spot size and gain of the PHFXRL.

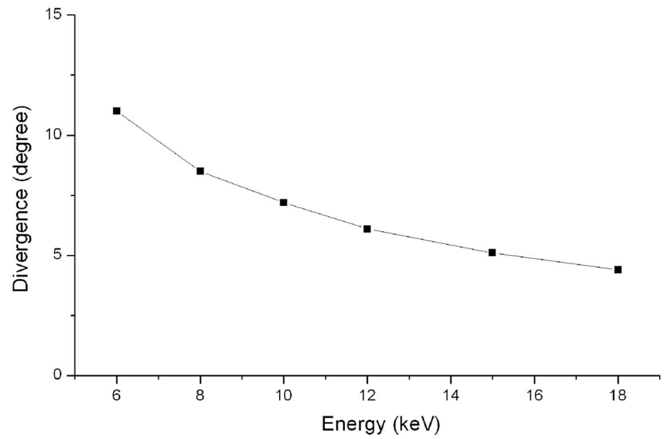

Figure 4
Energy dependence of the divergence of the PHFXRL.

As shown in Fig. 1, the magnification M of the X-ray image obtained using the system based on the polycapillary is given by

$$M = \frac{i + o}{o}, \qquad (2)$$

where o and i are the object–source and image–source distances, respectively.

2.3. Application of the imaging system

Images of a Ni film that was lithographically prepared for use as a test sample were obtained using the imaging system both with and without the PHFXRL. When the image was recorded with the PHFXR, the values of o and i (see Fig. 1) were 3.5 and 18.6 cm, respectively, giving $M = 6.3$. When the image was recorded using the quasi-parallel synchrotron radiation without the PHFXRL, the Ni film and the CCD were not moved, *i.e.* the value of i in Fig. 1 was not changed. Fig. 5 shows images of the Ni film recorded with and without the PHFXRL; Figs. 5(*b*) and 5(*c*) are original images with and without the PHFXRL, respectively, and Figs. 5(*a*) and 5(*d*) are the magnified images of Figs. 5(*b*) and 5(*c*) with a magnification of 1.6 and 6.5,

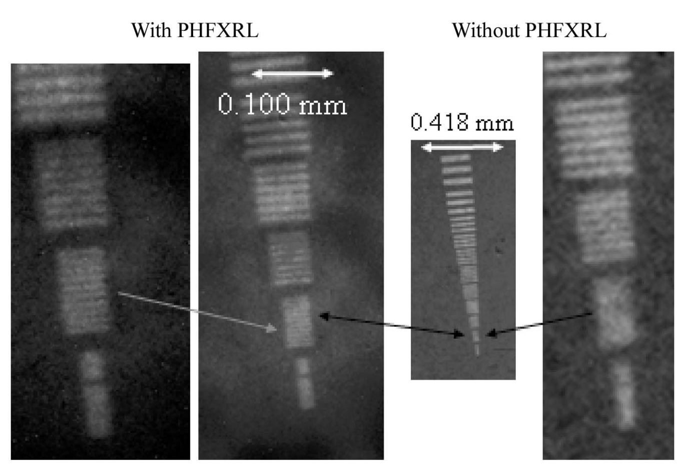

(*a*) (*b*) (*c*) (*d*)

Figure 5
Images of the Ni film recorded with and without the PHFXRL.

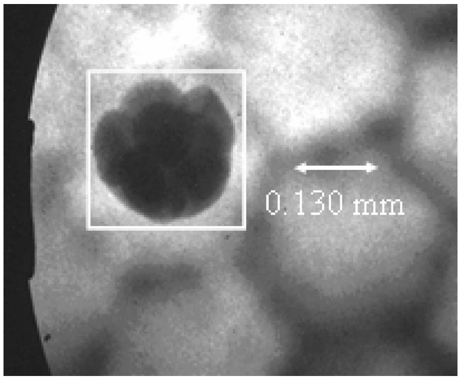

Figure 6
Image of an ancient fossil.

respectively, for visual clarity. As shown in the figure, the line of width 5 µm identified by the arrow can be seen in the image recorded using the PHFXRL.

To demonstrate the ability of the microscope to image a small sample, an image of an ancient fossil was obtained using this system with the PHFXRL and is presented in Fig. 6. The size of this fossil was about 338 µm in diameter. The values of o and i (see Fig. 1) were 3.1 and 12.6 cm, respectively, giving a magnification of $M = 5.1$. In recent years X-ray imaging studies on fossils have become increasingly popular (Chen *et al.*, 2006). Our future plans are to obtain three-dimensional structures by computed tomography using this system based on the PHFXRL.

3. Discussion

As shown in Figs. 5(*b*) and 6, there is a weak 'hexagon' pattern background in the images. This pattern is caused by the walls between the compound polycapillaries as shown in Fig. 2(*b*). This hexagon pattern can be removed by digitally subtracting the 'flat field' radiographs taken without samples.

If the walls between the compound polycapillaries are thick enough to totally filter the incident X-rays, the corresponding hexagon background pattern will seriously affect the quality of images of samples. Therefore, the PHFXRL used in such imaging experiments must have thin walls between the compound polycapillaries. We plan to improve the structure of the PHFXRL in order to obtain homogeneous radiation transmission and, accordingly, avoid the hexagon background.

4. Conclusions

A PHFXRL can provide a significant gain in flux density in its focal spot and relatively large divergence after its focal spot, which is suitable for magnifying the X-ray images of objects. The imaging system based on the PHFXRL has potential application in the area of imaging studies on small samples.

This research was supported by both the Key Project of Chinese Ministry of Education (108125) and Beijing Key Laboratory of Applied Optics (JD100270543).

References

Bulska, E. W., Wierzbicka, I. A., Małgorzata, H., Proost, K., Janssens, K. & Falkenberg, G. (2006). *Anal. Chem.* **78**, 7616–7624.
Chen, J.-Y., Bottjer, D. J., Davidson, E. H., Dornbos, S. Q., Gao, X., Yang, Y.-H., Li, C.-W., Li, G., Wang, X. Q., Xian, D.-C., Wu, H.-J., Hwu, Y.-K. & Tafforeau, P. (2006). *Science*, **312**, 1644–1646.
Dabagov, S. B., Kumakhov, M. A., Nikitina, S. V., Murashova, V. A., Fedorchuk, R. V. & Yakimenko, M. N. (1995). *J. Synchrotron Rad.* **2**, 132–135.
Gary, C. K., Park, H., Lombardo, L. W., Piestrup, M. A., Cremer, J. T., Pantell, R. H. & Dudchik, Y. I. (2007). *Appl. Phys. Lett.* **90**, 181111.
Janssensa, K., Proosta, K. & Falkenberg, G. (2004). *Spectrochim. Acta*, B**59**, 1637–1645.
Mokso, R., Cloetens, P., Maire, E., Ludwig, W. & Buffière, J.-Y. (2007). *Appl. Phys. Lett.* **90**, 144104.
Ollinger, C., Fuhse, C., Kalbfleisch, S., Tucoulou, R. & Salditt, T. (2007). *Appl. Phys. Lett.* **91**, 051110.
Piestrup, M. A., Gary, C. K., Park, H., Harris, J. L., Cremer, J. T., Pantell, R. H., Dudchik, Y. I., Kolchevsky, N. N. & Komarov, F. F. (2005). *Appl. Phys. Lett.* **86**, 131104.
Sun, T. & Ding, X. (2004). *Nucl. Instrum. Methods Phys. Res. B*, **226**, 651–658.
Sun, T. & Ding, X. (2005). *J. Appl. Phys.* **97**, 124904.
Sun, T., Liu, Z., He, B., Wei, S., Xie, Y., Liu, T., Hu, T. & Ding, X. (2007). *Nucl. Instrum. Methods Phys. Res. A*, **574**, 285–288.
Sun, T., Xie, Y., Liu, Z., Liu, T., Hu, T. & Ding, X. (2006). *J. Appl. Phys.* **99**, 094907.
Woll, A. R., Mass, J., Bisulca, C., Huang, R., Bilderback, D. H., Gruner, S. & Gao, N. (2006). *Appl. Phys. A*, **83**, 235–238.